

A NOVEL, ROBUST, HARMONIC INJECTION METHOD FOR SINGLE-SWITCH, THREE-PHASE, DISCONTINUOUS-CONDUCTION-MODE BOOST RECTIFIERS

Yungtaek Jang and Milan M. Jovanović

DELTA Power Electronics Lab., Inc.

1872 Pratt Drive, Suite 1400

Blacksburg, VA 24060

Abstract - This paper describes a new, robust, low-cost, harmonic-injection method for single-switch, three-phase, discontinuous-conduction-mode (DCM) boost rectifiers. In the proposed method, a periodic voltage is injected in the control circuit to vary the duty cycle of the rectifier switch within a line cycle so that the 5th-order harmonic of the input current is reduced to meet the IEC555-2 requirement. Since the injected voltage signal, which is proportional to the inverted ac component of the rectified three-phase line-to-line input voltages, is employed, the injected duty-cycle variations are naturally synchronized with the three-phase, line-to-neutral input voltages. In addition, the injected harmonic signal naturally contains desirable higher-order harmonics, such as 6th, 12th, 18th, etc., which are more effective in improving THDs than harmonic-injection methods based on the 6th-order harmonic only.

I. Introduction

The DCM, pulse-width-modulated (PWM), high-power-factor, boost rectifier for three-phase applications was introduced and analyzed in [1]. The major advantages of this rectifier are that its input-current waveshape automatically follows the input-voltage waveshape, and that it can achieve extremely high efficiencies because the reverse-recovery-related losses of the boost diode are eliminated. However, if the rectifier is implemented with the conventional low-bandwidth, output-voltage feedback control at a constant switching frequency, which keeps the duty cycle of the switch constant during a rectified line period, the rectifier input current exhibits a relatively large 5th-order harmonic. As a result, at power levels above 5 kW, the 5th-order harmonic imposes severe design, performance, and cost trade-offs in order to meet the maximum permissible harmonic-current levels defined by the IEC555-2 document [2]. Namely, to meet the IEC555-2 specifications at input-power levels above 5 kW, the DCM boost rectifier must be designed with the output voltage much higher than the peak of the input voltage [3]. Inevitably, such designs require higher voltage-rated switches, which are more expensive and usually have more losses than their counterparts with lower voltage ratings. Generally, to reduce the 5th-order harmonic and to improve THDs of the input currents, the duty cycle of the rectifier switch needs to be properly modulated during a rectified line period instead of being kept constant.

Recently, a number of duty-cycle modulation techniques for the DCM boost rectifier have been introduced to reduce the 5th-order harmonic of the input current and to improve THDs so that the power level at which the input-current-harmonic content still meets the IEC555-2 standard is extended [3] - [6]. Specifically, the approach based on the variable-switching-frequency control was

presented and analyzed in [4] and [5]. However, since the switching frequency of these rectifiers directly depends on the input voltage and output power variations, this technique suffers from a very wide switching-frequency range which decreases the efficiency and makes the rectifier design, device selection, and control circuit more complex.

To improve the performance of the DCM boost rectifier at a constant switching frequency, 6th-harmonic injection methods have been introduced in [3] and [6]. The injected 6th-harmonic signal modifies the duty cycle of the rectifier switch so that the 5th-order harmonic of the input current and the overall THDs are reduced to meet the IEC555-2 requirements. However, if the phase of the injected 6th-harmonic signal is not well synchronized with the 5th-order harmonic of the input current, the expected reduction of the 5th-order harmonic and the improvement of the THDs cannot be achieved. For example, the proposed 6th-harmonic injection circuit in [3], which employs a bandpass filter, has a severe phase shift problem which requires phase-detecting and phase-locking circuits for reliable operation. In fact, the harmonic-injection technique which utilizes the voltage ripple of the rectifier output voltage and employs phase-detecting and phase-locking circuits to properly synchronize the injected signal with the rectifier input currents is proposed in [6].

In this paper, a robust, low-cost, harmonic-injection method for the single-switch, three-phase, DCM boost rectifier and its implementations are presented. To reduce the 5th-order harmonic and improve THDs of the rectifier input currents, a periodic voltage signal is injected to vary the duty cycle of the rectifier within a line cycle. The proposed harmonic-injection technique uses a voltage

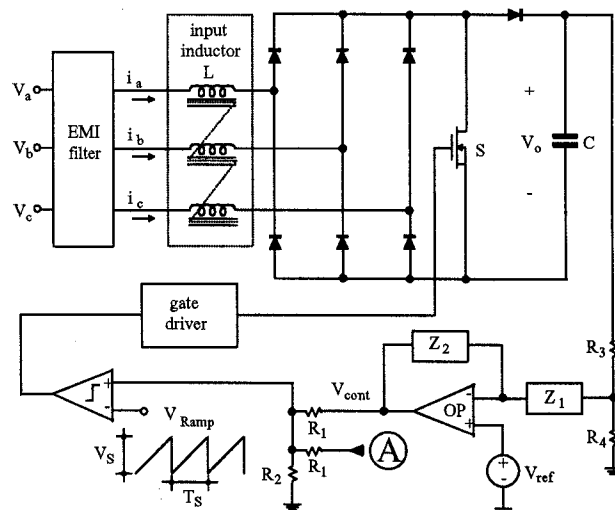


Fig. 1: Conventional, single-switch, three-phase, DCM boost rectifier.

signal which is proportional to the inverted ac component of the rectified, three-phase, line-to-line input voltages. As a result, the injected signal is naturally synchronized with the three-phase, line-to-neutral input voltages. Moreover, the closed-loop feedback control of the DCM boost rectifier is not affected by the proposed open-loop harmonic-injection method.

II. Brief Review of Operation and Input-Current-Harmonic Analysis of Three-Phase, PWM, DCM Boost Rectifiers

In this section, a brief review of the operation and input-current harmonic-content analysis of the single-switch, three-phase, PWM, DCM boost rectifier, shown in Fig. 1, is presented, assuming that:

- the rectifier operates in DCM.
- Switching frequency f_s is much higher than line frequency f_L .
- The three-phase input voltages are well balanced undistorted sinewaves.
- The input voltage can be considered constant during a switching interval.
- The output voltage and the output current are approximately constant.
- All semiconductor components are ideal.
- There are no power losses in the converter.

Since the boost rectifier is operated in DCM with a constant frequency and constant duty cycle, all three-phase input currents, i_a , i_b , and i_c , are zero at the end of a switching period, immediately before boost switch S is turned on. After switch S is turned on, i_a , i_b , and i_c increase linearly to the peak values which are proportional to the line-to-neutral voltages, as shown in Fig. 2. Therefore, during the switch-on period of the rectifier, each line current forms a triangular pulse with the peak value proportional to the associated line-to-neutral voltage. As a result, during the switch-on period, the average line currents are proportional to the line-to-neutral voltages. When the switch is turned off, the input currents start decreasing because output voltage V_o is higher than the peak of the input voltage. In DCM, the input currents reach zero before the end of the switching period. Since the rate of the input-current decrease is proportional to the difference between output voltage V_o and line-to-neutral voltage, the average line currents during the switch-off period are not proportional to the line voltages, *i.e.*, even if the line voltages are perfectly balanced and sinusoidal, the line currents are distorted.

The average line currents during a switching period of a constant-frequency, constant-duty-cycle, DCM boost rectifier were derived in [1] and [5]. The derivations assume that switching frequency f_s is much higher than line frequency f_L ; the well balanced and

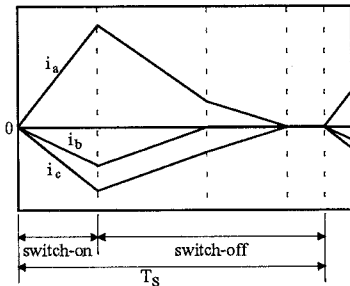


Fig. 2: Input currents i_a , i_b , and i_c of the conventional, single-switch, three-phase, DCM boost rectifier. The currents are drawn assuming $V_o > 0$, $V_c < V_o < 0$.

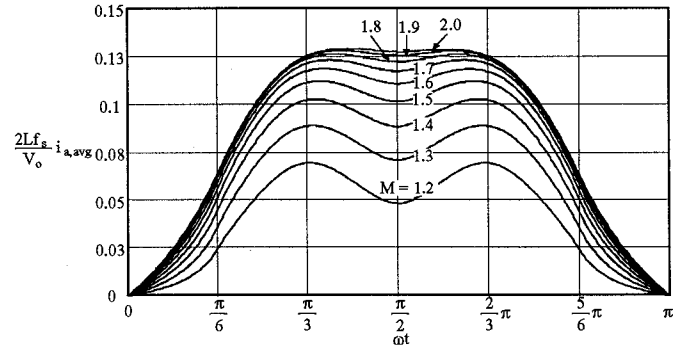


Fig. 3: Normalized, average input current $i_{a,avg}$ of the conventional, single-switch, three-phase, DCM boost rectifier for different voltage-conversion ratios M .

undistorted three-phase input voltages can be considered constant within each switching cycle, *i.e.*:

$$V_a = V_m \sin(\omega t), \quad (1)$$

$$V_b = V_m \sin\left(\omega t - \frac{2\pi}{3}\right), \quad (2)$$

$$V_c = V_m \sin\left(\omega t - \frac{4\pi}{3}\right), \quad (3)$$

where V_m is the peak line-to-neutral voltage and $\omega = 2\pi f_L$ is angular line-frequency. According to [1] and [5], the average input currents over a switching period are given by:

$$i_{a,avg} = \frac{V_o D^2}{2L f_s} \frac{\sin(\omega t)}{\sqrt{3M - 3\sin(\omega t)}} \quad \left(0 \leq \omega t \leq \frac{\pi}{6}\right), \quad (4)$$

$$i_{a,avg} = \frac{V_o D^2}{2L f_s} \frac{M \sin(\omega t) + \frac{1}{2} \sin\left(2\omega t - \frac{2\pi}{3}\right)}{\left[\sqrt{3M - 3\sin\left(\omega t + \frac{2\pi}{3}\right)}\right] \left[M - \sin\left(\omega t + \frac{\pi}{6}\right)\right]} \quad \left(\frac{\pi}{6} \leq \omega t \leq \frac{\pi}{3}\right), \quad (5)$$

$$i_{a,avg} = \frac{V_o D^2}{2L f_s} \frac{M \sin(\omega t) + \sin\left(2\omega t + \frac{\pi}{3}\right)}{\left[\sqrt{3M + 3\sin\left(\omega t + \frac{2\pi}{3}\right)}\right] \left[M - \sin\left(\omega t + \frac{\pi}{6}\right)\right]} \quad \left(\frac{\pi}{3} \leq \omega t \leq \frac{\pi}{2}\right), \quad (6)$$

where V_o is the rectifier output voltage, D is the duty ratio, L is the inductance of the input inductors, and M is the voltage conversion ratio defined as

$$M = \frac{V_o}{\sqrt{3} V_m}. \quad (7)$$

From equations (4) - (7), the average input currents for different voltage-conversion ratios are calculated and plotted as shown in Fig. 3. The THDs and harmonic contents of the average input current for different values of M can be calculated by Fourier analysis. Figure 4 shows the normalized harmonic content of the rectifier input current as a function of M , whose practical range is from 1.2 to 2. As can be seen from Fig. 4, the rectifier input-current spectrum which contains only odd harmonics is dominated by the 5th-order harmonic, *i.e.*, the lowest order harmonic. For example, at $M = 1.2$, the 5th-order harmonic is 8 times larger than the 7th-order harmonic which is the next largest. Also, it should be noted that the value of the normalized 5th-order harmonic monotonically decreases as the values of M increase. In fact, it decreases from slightly over 40% of the fundamental component at $M = 1.1$ to approximately 7% at $M = 2$.

Generally, the maximum input power at which the three-phase, constant-frequency, DCM boost rectifier can meet the IEC555-2

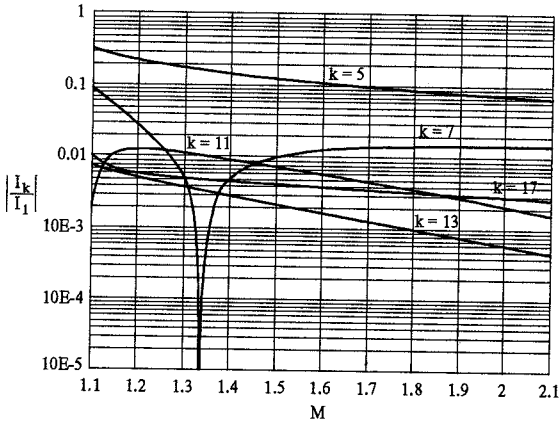


Fig. 4: Normalized input-current harmonics of the single-switch, three-phase, constant-frequency, constant-duty-cycle, DCM boost rectifier. Harmonics are normalized with respect to the fundamental component.

specifications is limited by the 5th-order harmonic of the input current. As an illustration, Fig. 5 shows the 5th, 7th, 11th, and 13th harmonics of the DCM boost rectifier with $M = 1.4$ and input power levels from 5 kW to 10 kW, along with the corresponding IEC555-2 limits. As can be seen from Fig. 5, for $M = 1.4$ the rectifier can meet the IEC555-2 requirements only for power levels up to 5 kW because of the 5th-harmonic limitation. The higher-order harmonics, *i.e.*, 7th, 11th, 13th, etc., are well below the IEC555-2 limits, even for power levels over 10 kW.

To meet the IEC555-2 specifications at power levels above 5 kW, the three-phase, constant-frequency, constant-duty-cycle DCM boost rectifier needs to be designed with a higher M [3]. However, it should be noted that for a given power line voltage, larger M requires a boost switch with a higher voltage rating. Therefore, to maximize the efficiency and reduce the cost, the design with the minimum M which meets the specifications such as IEC555-2 or desired THDs should be used.

Since the 5th-order harmonic is the dominant harmonic in the input-current spectrums, as shown in Fig. 4, the three-phase input currents of the constant-switching-frequency, constant-duty-ratio, DCM boost rectifier can be approximated by neglecting the higher-order harmonics as

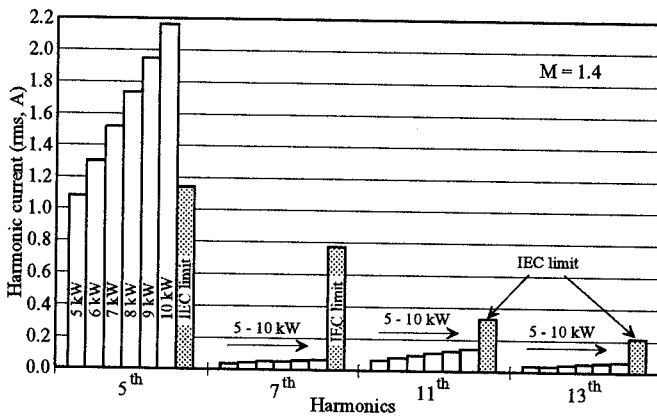


Fig. 5: Comparison between input-current harmonic content of the DCM boost rectifier and harmonic-current limits of the IEC555-2 for $M = 1.4$, $V_{out} = 750$ V, $V_{in(L-L)} = 380$ V_{rms}, $P_{in} = 5$ kW - 10 kW.

$$i_{a,avg} = I_1 \sin(\omega t) - I_5 \sin(5\omega t), \quad (8)$$

$$i_{b,avg} = I_1 \sin\left(\omega t - \frac{2\pi}{3}\right) - I_5 \sin\left(5\omega t - \frac{2\pi}{3}\right), \quad (9)$$

$$i_{c,avg} = I_1 \sin\left(\omega t - \frac{4\pi}{3}\right) - I_5 \sin\left(5\omega t - \frac{4\pi}{3}\right). \quad (10)$$

III. New, Low-Cost, Injection-Signal Generators

In the circuit proposed in this paper, a signal proportional to the inverted ac component of the three-phase, line-to-line, input voltages is injected into the control circuit at node A in Fig. 1 to modulate the duty cycle of the boost rectifier switch and reduce the 5th-order harmonic of the line current. Two implementations of the injection-signal generator are described in this paper. One implementation uses three low-frequency, step-down transformers to generate the injection signal; the other implementation does not require the transformers, but instead employs three operational amplifiers (op-amps) to accomplish the same task.

A. Implementation with transformers

The circuit diagram of the injection-signal generator implemented with three low-frequency, step-down transformers, along with its key waveforms, is shown in Fig. 6. Besides the three transformers, the circuit in Fig. 6(a) also incorporates three-phase diode bridge BR, blocking capacitor C_b , and an op-amp with a feedback network (Z_{f1} and Z_{f2}). Three low-frequency transformers are utilized for the voltage step-down and isolation between the injection circuit and the power stage. The primary terminals of the step-down transformers are connected to the line-to-line input voltages V_{ab} , V_{bc} , and V_{ca} . The secondary-side voltages of the

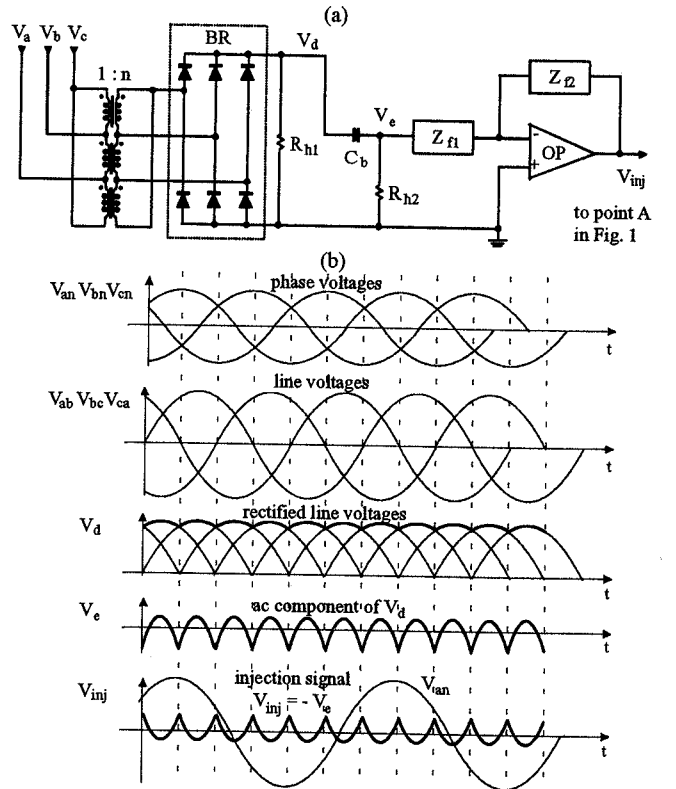


Fig. 6: Injection circuit with isolation transformers: (a) schematic diagram; (b) key voltage waveforms.

transformers are rectified by three-phase diode bridge BR. The dc component of rectified voltage V_d is eliminated by blocking capacitor C_b . Since the impedance of C_b at the line frequency is much smaller than R_{L2} , the voltage across R_{L2} is nearly identical to the ac component of V_d . Finally, the polarity of the voltage signal V_e is inverted by the op-amp so that the desired injection signal V_{inj} , shown in Fig. 6(b), is obtained.

Since the proposed injection-signal generator does not contain a bandpass filter but only a high-pass filter with the corner frequency well below the frequency of the 6th-order harmonic, the injection-signal which contains 6th and higher-order harmonics does not suffer from any significant delay. As a result, the injection signal V_{inj} phase is naturally well synchronized with all the input currents and line-to-neutral voltages. Moreover, this phase synchronization does not drift with time and it is not very sensitive to component tolerances.

When signal V_{inj} , shown in Fig. 6 (b), is injected at the input of the PWM modulator (node A in Fig. 1), it modifies the duty cycle so that the 5th-order harmonic of the input current is reduced and the THDs are improved. In fact, since the variation of duty cycle $d(t)$ is directly proportional to the injected signal V_{inj} , the modulation of duty ratio during a line cycle can be described as

$$D_{MOD}(t) = D[1 + d(t)], \quad (11)$$

where D_{MOD} is the modulated duty cycle, D is the duty cycle in the absence of the modulation, and $d(t)$ is the duty cycle modulation. Since $d(t)$ is proportional to the inverted ac component of the rectified three-phase line-to-line input voltages, the variation of duty cycle $d(t)$ during a half of the fundamental line period can be plotted along with the line-to-neutral input voltage, as shown in Fig. 7. Moreover, $d(t)$ can be described as a function of modulation factor m and angular line frequency ωt for the first quarter of the fundamental period ($0 < \omega t < \pi/2$) as

$$d(t) = -m \left[\cos(\omega t) - \frac{6}{\pi} \cos \frac{\pi}{3} \right] \quad \left(0 \leq \omega t \leq \frac{\pi}{6} \right), \quad (12)$$

$$d(t) = -m \left[\cos \left(\omega t - \frac{\pi}{3} \right) - \frac{6}{\pi} \cos \frac{\pi}{3} \right] \quad \left(\frac{\pi}{6} \leq \omega t \leq \frac{\pi}{2} \right), \quad (13)$$

where m is the modulation factor defined as

$$m = \sqrt{3} V_m \times n \times \frac{Z_{r2}}{Z_{r1}} \times \frac{1}{V_{cont}}. \quad (14)$$

As shown in Fig. 6, n is the transformer turns ratio and Z_{r2}/Z_{r1} is the feedback gain of the op-amp, while V_m is the peak line-to-neutral input voltage, and V_{cont} is the output voltage of the gain compensator shown in Fig. 1. It should be noted that the expressions for $d(t)$ given in Eqs. (12) and (13) are valid for a quarter of the fundamental period ($0 < \omega t < \pi/2$). However, they can be easily extended to a whole line period because of the waveform symmetry.

The periodic function described by Eqs. (12) and (13) can be

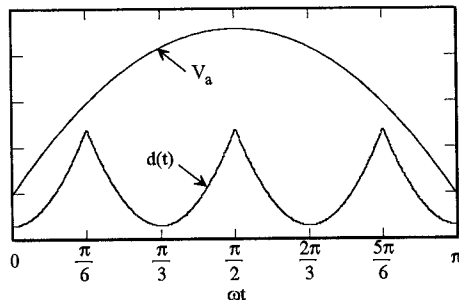


Fig. 7: Duty-cycle variations during a half of the fundamental line period.

expressed in terms of the Fourier series representation as

$$d(t) = \frac{m}{\pi} \sum_{n=1}^{\infty} \frac{(-1)^n 6}{(6n)^2 - 1} \cos(6n\omega t). \quad (15)$$

From Eq. (15), it can be seen that the generated injection signal contains not only the 6th-order harmonic but also higher-order harmonics such as 12th, 18th, etc.. These higher-order harmonics help improve THDs more than if only the 6th-order harmonic is injected.

By substituting D in Eqs. (4) - (6) with the modified duty ratio D_{MOD} defined in Eq. (11), the average input current $i_{a,avg}^{inj}$ in the presence of the signal injection can be described as

$$i_{a,avg}^{inj} = i_{a,avg} (1 + d(t))^2 \approx i_{a,avg} (1 + 2d(t)), \quad (16)$$

where $d(t)^2$ term is neglected, since it is much smaller than the unity.

Using Eqs. (8) and (15), the average input current $i_{a,avg}^{inj}$ defined in Eq. (16) can be calculated as

$$i_{a,avg}^{inj} = (I_1 - qI_5) \sin(\omega t) - (I_5 - qI_1) \sin(5\omega t) - \left(qI_1 - \frac{35}{143} qI_5 \right) \sin(7\omega t) \\ + \left(qI_5 - \frac{35}{143} qI_1 \right) \sin(11\omega t) + \left(\frac{35}{143} qI_1 - \frac{35}{323} qI_5 \right) \sin(13\omega t) \dots, \quad (17)$$

where the constant q is defined as

$$q = \frac{6}{35\pi} m, \quad (18)$$

i.e., it is proportional to modulation index m .

Similarly, the input currents $i_{b,avg}^{inj}$ and $i_{c,avg}^{inj}$ can also be calculated as

$$i_{b,avg}^{inj} = (I_1 - qI_5) \sin \left(\omega t - \frac{2\pi}{3} \right) + (I_5 - qI_1) \sin \left(5\omega t + \frac{\pi}{3} \right) \\ + \left(qI_1 - \frac{35}{143} qI_5 \right) \sin \left(7\omega t + \frac{\pi}{3} \right) + \left(qI_5 - \frac{35}{143} qI_1 \right) \sin \left(11\omega t - \frac{2\pi}{3} \right) \dots, \quad (19)$$

$$i_{c,avg}^{inj} = (I_1 - qI_5) \sin \left(\omega t - \frac{4\pi}{3} \right) + (I_5 - qI_1) \sin \left(5\omega t - \frac{\pi}{3} \right) \\ + \left(qI_1 - \frac{35}{143} qI_5 \right) \sin \left(7\omega t - \frac{\pi}{3} \right) + \left(qI_5 - \frac{35}{143} qI_1 \right) \sin \left(11\omega t - \frac{4\pi}{3} \right) \dots. \quad (20)$$

Therefore, from Eqs. (17) - (20), the THDs of the input currents of the three-phase, constant-frequency, DCM, boost rectifier with the proposed harmonic-injection control is given by

$$THDs = \frac{\sqrt{(I_5 - qI_1)^2 + \left(qI_1 - \frac{35}{143} qI_5 \right)^2 + \left(qI_5 - \frac{35}{143} qI_1 \right)^2} \dots}{I_1 - qI_5}. \quad (21)$$

From Eqs. (17) - (21), it can be seen that, for a given voltage conversion ratio, the THDs are a function of modulation index m .

At any given voltage-conversion ratio M , optimal modulation

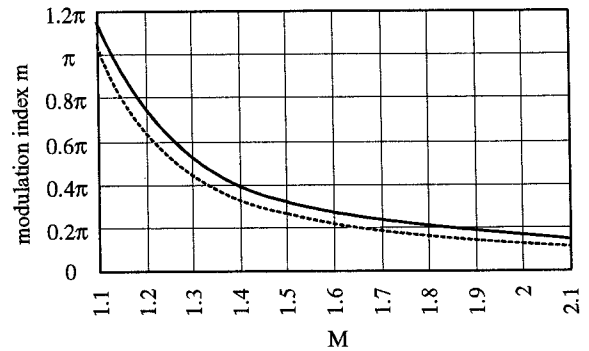


Fig. 8: Optimal modulation index m versus voltage conversion ratio M for the minimum THDs (solid line) and for the maximum output power (dashed line).

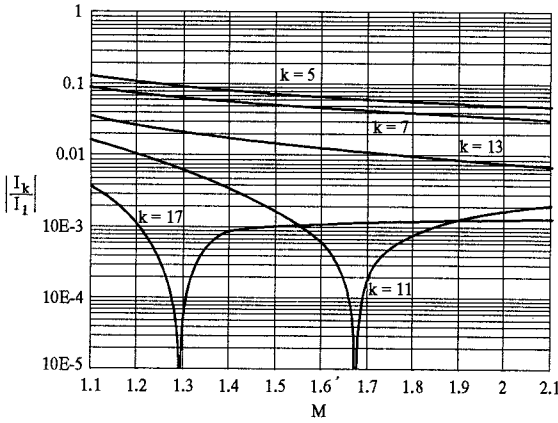


Fig. 9: Normalized input-current harmonics of the single-switch, three-phase, DCM boost rectifier with the proposed harmonic-injection control. Harmonics are normalized with respect to the fundamental component.

index m which produces the minimum THDs can be determined from Eqs. (18) and (21). Figure 8 shows the calculated values of optimal modulation index m for the minimum THDs (solid line) as a function of M . To maximize the input power of the rectifier at which the IEC555-2 specifications are met, modulation index m should be determined so that the ratio of the 7th-order harmonic and the 5th-order harmonic is equal to corresponding IEC555-2 limits, *i.e.*,

$$\left| \frac{qI_1 - \frac{35}{143}qI_5}{I_5 - qI_1} \right| = \frac{0.77 \text{ A}}{1.14 \text{ A}} = 0.675, \quad (22)$$

where 1.14 A and 0.77 A are IEC555-2 limits for the 5th-order harmonic and the 7th-order harmonic, respectively. It should be noted that the effects of the higher-order harmonics are not significant in comparison with the 5th and 7th-order harmonics. Moreover, the higher frequency harmonics can be easily eliminated by an EMI input filter. Figure 8 shows the calculated values of optimal modulation index m for the maximum input power (dashed line) as a function of M .

Using the optimal modulation index m for the maximum input power, a normalized harmonic content of the rectifier input current can be calculated as shown in Fig. 9. It can be seen that the

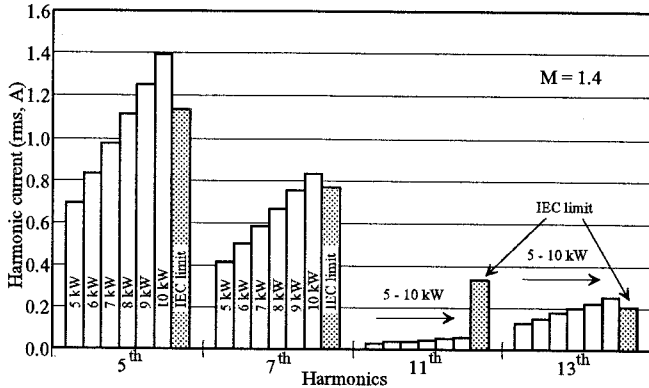


Fig. 10: Comparison between input-current harmonic content of the DCM boost rectifier with the proposed harmonic injection and harmonic-current limits of the IEC555-2 for $M = 1.4$, $V_{\text{out}} = 750 \text{ V}$, $V_{\text{in(L-L)}} = 380 \text{ V}_{\text{rms}}$, $P_{\text{in}} = 5 \text{ kW} - 10 \text{ kW}$.

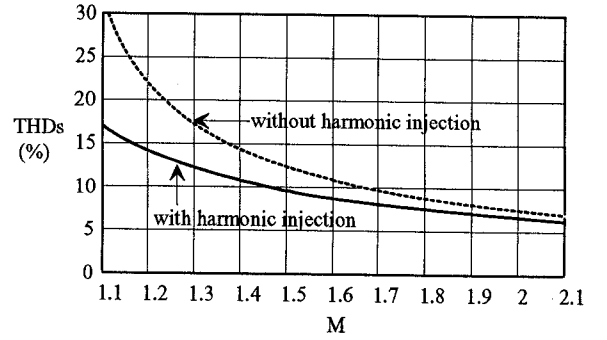


Fig. 11: Input-current THDs as functions of the voltage-conversion ratio of a constant-frequency, DCM boost rectifier with constant duty cycle (dashed line) and with modulated duty cycle using the proposed harmonic-injection method (solid line).

magnitudes of the 5th, 7th, and 13th harmonics are linearly proportional to one another.

Figure 10 shows the estimated normalized 5th, 7th, 11th, and 13th harmonics of the input current of the DCM boost rectifier with harmonic-injection control for input power levels from 5 kW to 10 kW. The harmonics are obtained by assuming that line-to-line input voltage $V_{\text{in(L-L)}} = 380 \text{ V}_{\text{rms}}$ and output voltage $V_o = 750 \text{ V}_{\text{dc}}$, *i.e.*, assuming $M = V_o / \sqrt{3}V_{\text{in}} = 1.4$. The IEC555-2 limits for each of the harmonics are also shown in Fig. 10. As can be seen from Fig. 10, employing the proposed injection method, the maximum power of the rectifier at which the IEC555-2 requirements are met is extended to 8 kW. As shown in Fig. 5, the corresponding maximum power for the rectifier without harmonic injection at $M = 1.4$ is only about 5 kW.

Finally, the comparison between the THDs of the constant-switching-frequency, DCM boost rectifier without and with the proposed harmonic injection is given in Fig. 11. As can be seen from Fig. 11, the reduction of the THDs with the proposed injection technique is the most significant for $M < 1.4$. Specifically, for $M < 1.4$, the reduction in the THDs is at least 5%. For larger values of M , the injection approach is less effective. For example, for $M = 2$, the reduction of the THDs of the circuit with the injection is less than 1% in comparison with that without the injection.

B. Implementation without transformers

The injection signal generator can also be implemented without bulky, low-frequency, step-down transformers, as shown in Fig. 12. The circuit in Fig. 12 employs resistive voltage dividers $R_a - R_c$ and op-amps OP1 - OP3 configured as difference amplifiers to step-down the three-phase input voltages to the desired level. Namely, the Y-connected resistive voltage dividers $R_a - R_c$ are connected to the line-to-line input voltages V_{ab} , V_{bc} , and V_{ca} . The step-down line-to-neutral voltages across resistor R_c are then processed by op-amps OP1 - OP3 which are referenced to the control ground. It should be noted that the control ground is isolated from the ground of three-phase input voltages by $R_a = 4 \text{ M}\Omega$ resistors. The output voltages of the difference amplifiers are further rectified by three-phase bridge BR. The dc component of rectified voltage V_d is then eliminated by the blocking capacitor C_b . Since the impedance of the blocking capacitor C_b at the line frequency is much smaller than R_{b2} , the voltage across R_{b2} is nearly identical to the ac component of V_d . Finally, the polarity of the voltage signal V_c is inverted by difference amplifier OP4 so that signal V_{inj} has the desired polarity.

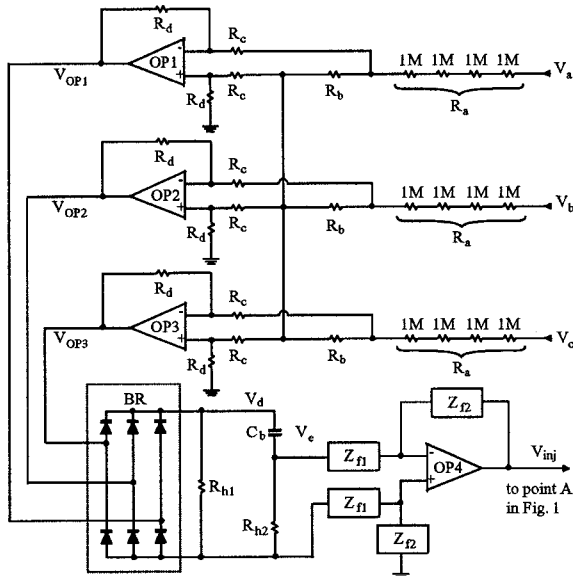


Fig. 12: Schematic diagram of the harmonic-injection circuit with difference op-amps. The key circuit waveforms are the same as in Fig. 6(b).

As in the case of the implementation with the transformers, voltage signal V_{inj} is naturally in phase with all input currents and line-to-neutral voltages. The performance of the circuit in Fig. 12 is identical to that of the circuit in Fig. 6. However, the injection circuit shown in Fig. 12 has a smaller size, and is less expensive than the circuit shown in Fig. 6.

IV. Experimental Results

To verify the performance of the proposed injection technique, a three-phase, 6-kW, DCM boost rectifier for the 304 V_{rms} - 456 V_{rms} line-to-line input voltage range (380 $V_{rms} \pm 20\%$) and $V_o = 750 V_d$ was built. The circuit diagram of the power stage is given in Fig. 13. The rectifier was designed with a constant switching frequency of 45 kHz.

Figure 14 shows the oscillograms of input voltage and current waveforms of the experimental circuit without harmonic-injection control at full power and different input voltages, while Fig. 15 shows the measured input-current harmonics under the same conditions. As can be seen from Fig. 15, the 5th-order harmonic of the input current is over the IEC555-2 limit for the nominal input voltage (380 V_{rms}) and higher.

To evaluate the performance of the proposed injection approach,

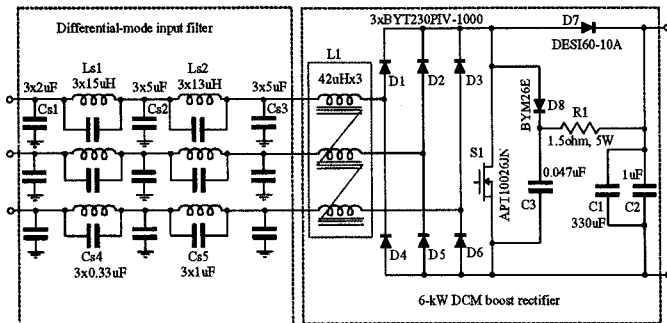


Fig. 13: Schematic diagram of the 6-kW, single-switch, 3-φ, DCM boost rectifier.

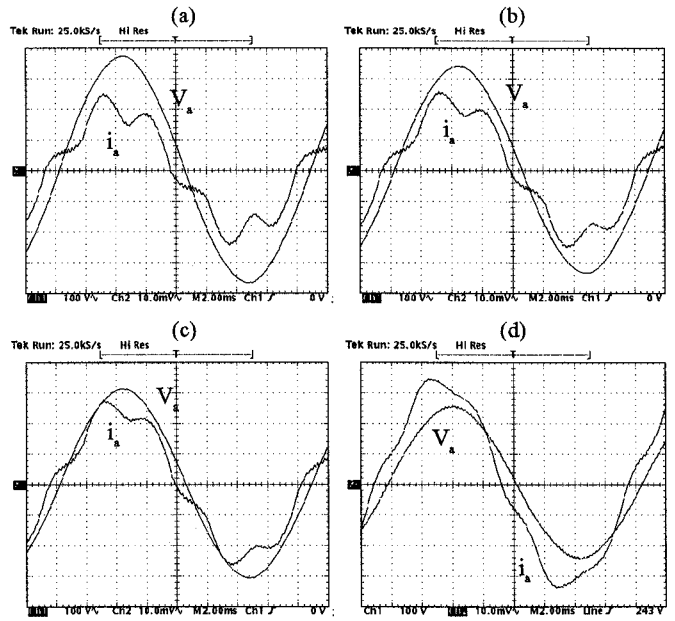


Fig. 14: Input voltage V_a (100 V/div) and input current i_a (5 A/div) waveforms of the experimental, 6-kW, DCM boost rectifier without harmonic-injection control at: (a) $V_{in(LL)} = 456 V_{rms}$, (b) 417 V_{rms} , (c) 380 V_{rms} , and (d) 304 V_{rms} .

both implementations of the injection circuit (with and without step-down transformers), shown in Figs. 6(a) and 12, were built. Figure 16 shows the oscillograms of input voltage and current waveforms of the experimental circuit with harmonic-injection control at full power and different input voltages.

The measured input-current harmonics of the experimental rectifier at full power and at different input voltages are summarized in Fig. 17. It should be noted that the measured performances of both implementations were also identical. As can be seen from Fig. 17, the magnitudes of the 5th-order harmonic as well as the higher harmonics are well below the IEC555-2 limit in the entire input voltage range (304 V_{rms} - 456 V_{rms}).

Finally, Table 1 shows the measured rms input-current harmonics at different input voltages, while Table 2 shows the full-power measured efficiency of the rectifier at the same range of input voltages. The rectifier exhibits the maximum efficiency of 98% at

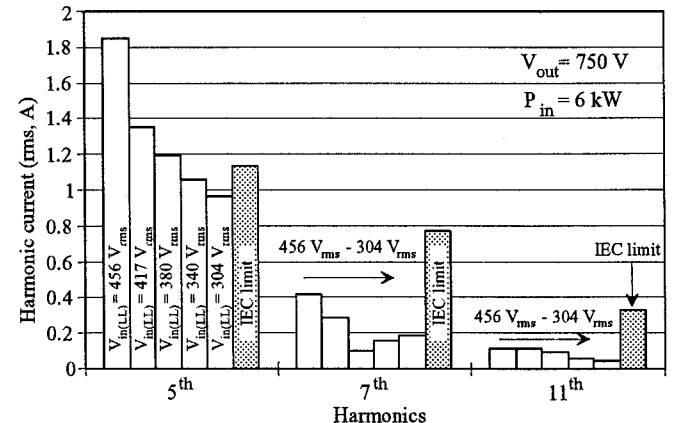


Fig. 15: Measured full-power input-current harmonics of the experimental DCM boost rectifier without harmonic-injection control at different input voltages.

the maximum input voltage of $456 V_{rms}$. The minimum efficiency of 96% occurs at lower line ($304 V_{rms}$).

Table 1: Measured input-current harmonics of the experimental, 6-kW, DCM, boost rectifier with the harmonic-injection control at full-power and different input voltages.

harmonic number	three-phase input voltages					IEC555-2 limits
	$456 V_{rms(LL)}$	$417 V_{rms(LL)}$	$380 V_{rms(LL)}$	$340 V_{rms(LL)}$	$304 V_{rms(LL)}$	
1	7.72 A	8.4 A	9.19 A	10.28 A	11.3 A	
3	0.12 A	0.12 A	0.08 A	0.09 A	0.06 A	2.3 A
5	1.01 A	0.78 A	0.74 A	0.61 A	0.59 A	1.14 A
7	0.49 A	0.63 A	0.56 A	0.65 A	0.60 A	0.77 A
9	0.04 A	0.02 A	0.02 A	0.01 A	0.02 A	0.4 A
11	0.07 A	0.08 A	0.02 A	0.01 A	0.02 A	0.33 A
2	0.18 A	0.15 A	0.13 A	0.12 A	0.11 A	1.08 A
4	0.22 A	0.2 A	0.17 A	0.16 A	0.14 A	0.43 A
6	0.01 A	0.01 A	0.00 A	0.01 A	0.01 A	0.3 A
8	0.01 A	0.04 A	0.01 A	0.02 A	0.01 A	0.23 A
10	0.05 A	0.01 A	0.03 A	0.01 A	0.01 A	0.184 A
THDs	15.74%	12.86%	10.93%	9.23%	7.52%	

Table 2: Measured full-power efficiency of the experimental, 6-kW, DCM, boost rectifier with the proposed harmonic-injection control at different input voltages.

input voltage [V]	input power [W]	output voltage [V]	output power [W]	loss [W]	efficiency [%]
456	5870	752	5759	111	98.1
417	5910	752	5772	138	97.7
380	5983	755	5815	168	97.2
340	5956	752	5756	200	96.6
304	5975	750	5740	235	96.1

* Input and output power measurements: Voltech PM3000A Universal Power Analyzer, PM1000 AC Power Analyzer

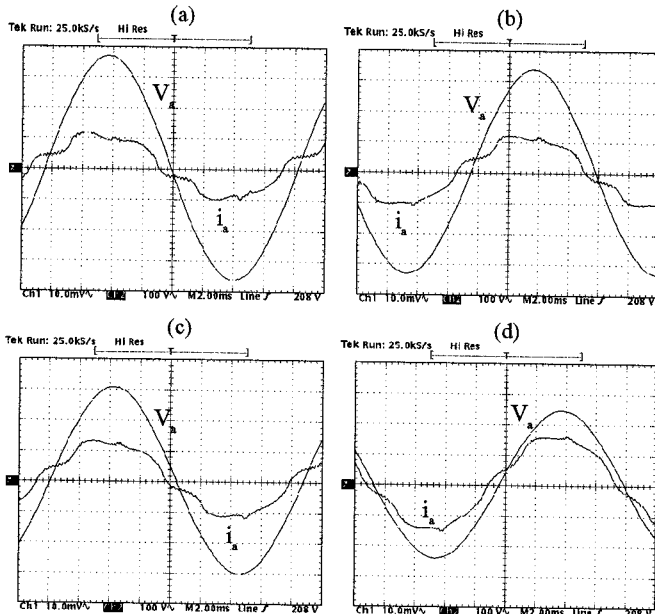


Fig. 16: Input voltage V_a (100 V/div) and input current i_a (10 A/div) waveforms of the experimental, 6-kW, DCM boost rectifier with the proposed harmonic-injection control at: (a) $V_{in(LL)} = 456 V_{rms}$, (b) $417 V_{rms}$, (c) $380 V_{rms}$, and (d) $304 V_{rms}$.

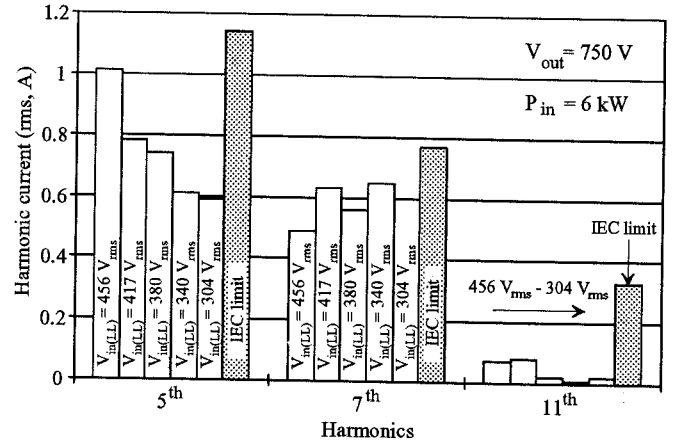


Fig. 17: Measured full-power input-current harmonics of the experimental DCM boost rectifier with harmonic-injection control at different input voltages.

V. Conclusions

In this paper, a new, robust, low-cost, harmonic-injection method for single-switch, three-phase, DCM boost rectifiers has been described. In the proposed method, a periodic voltage which is proportional to the inverted ac component of the rectified three-phase line-to-line input voltages is injected in the control circuit to vary the duty cycle of the rectifier switch within a line cycle so that the 5th-order harmonic of the input current is reduced to meet the IEC555-2 requirement. Moreover, the injected duty-cycle variations are naturally synchronized with the three-phase, line-to-neutral input voltages without using expensive phase-detecting and phase-locking circuits. The analysis of the injected signal and modified harmonic currents of the rectifier have been presented and verified on a laboratory prototype. The measured input-current harmonics of the 6-kW prototype rectifier were found to be well below the IEC555-2 limits over the entire input voltage range ($304 V_{rms} - 456 V_{rms}$). The rectifier efficiency is about 97% at full load and nominal line.

References

- [1] A. R. Prasad, P. D. Ziogas, and S. Manias, "An Active Power Factor Correction Technique for Three-Phase Diode Rectifiers," *IEEE Power Electronics Specialists Conf. (PESC) Record*, pp. 58 - 66, 1989.
- [2] International Electrotechnical Commission, Sub-Committee 77A, "Equipment Connection to the Public Low-Voltage Supply System", *Draft-Revision of IEC555-2: "Harmonic"*, Budapest, Oct., 1990.
- [3] Q. Huang and F. C. Lee, "Harmonic Reduction in A Single-Switch, Three-Phase Boost Rectifier with High Order Harmonic Injected PWM," *IEEE Power Electronics Specialists Conf. (PESC) Record*, pp. 1266 - 1271, 1996.
- [4] L. Simonetti, J. Sebastian, and J. Uceda, "Single-Switch Three-Phase Power Factor Under Variable Switching Frequency and Discontinuous Input Current," *IEEE Power Electronics Specialists Conf. (PESC) Record*, pp. 657 - 662, 1993.
- [5] J. W. Kolar, H. Ertl, and F. C. Zach, "Space Vector-Based Analytical Analysis of the Input Current Distortion of A Three-Phase Discontinuous-Mode Boost Rectifier System," *IEEE Power Electronics Specialists Conf. (PESC) Record*, pp. 696 - 703, 1993.
- [6] J. Sun, N. Frohlike, and H. Grotstollen, "Harmonic Reduction Techniques for Single-Switch Three-Phase Boost Rectifiers," *Conference Record of the 1996 IEEE Industry Applications Society Annual Meeting*, pp. 1225 - 1232, 1996.